



Australian Government
Department of Defence
Defence Science and
Technology Organisation

Evaluation of Pre-Built Space-Time Non-Adaptive Processing (PSTAP)

Yunhan Dong

Electronic Warfare and Radar Division
Defence Science and Technology Organisation

DSTO-RR-0295

ABSTRACT

Pre-built space-time non-adaptive processing (PSTAP) has been proposed in a previous DSTO report. This report further examines the performance of PSTAP using simulated airborne radar data generated by the Rome Laboratory Space-Time Adaptive Processing (RLSTAP) software. Results from the conventional STAP diagonally loaded sample matrix inversion (DL-SMI) method are used as benchmarks to evaluate results of PSTAP. It is found that PSTAP performs the same as STAP. Most importantly, PSTAP does not need computing computationally intensive optimum weights in real-time.

RELEASE LIMITATION

Approved for public release

Published by

*Electronic Warfare and Radar Division,
Defence Science and Technology Organisation
PO Box 1500
Edinburgh South Australia 5111 Australia*

*Telephone: (08) 8259 5555
Fax: (08) 8259 6567*

*© Commonwealth of Australia 2005
AR-013-463
July 2005*

APPROVED FOR PUBLIC RELEASE

Evaluation of Pre-Built Space-Time Non-Adaptive Processing (PSTAP)

Executive Summary

In scenarios where an airborne phased array Doppler radar is used in searching for moving targets whose signals are embedded in Gaussian distributed undesired signals including clutter (echoes from the terrain surface), noise jamming and thermal noise, space-time adaptive processing (STAP) provides the optimum signal-to-interference-and-noise ratio (SINR). However STAP normally requires the inverse of the covariance matrix (ICM) of undesired signals in order to form the optimum weights to process the received data. The typical dimension of the covariance matrix (CM) of undesired signals ranges from hundreds to thousands. It is this large computational load that prevents the implementation of fully adaptive STAP algorithms in real airborne radar systems at current computer speeds.

We have proven that the ICM is approximately invariant to changes in clutter returns. Based on this observation we have proposed pre-built space-time non-adaptive processing (PSTAP) in a previous DSTO Research Report. The approximate invariance of the ICM means that the ICM depends on radar and platform parameters, but is approximately independent of clutter environments. The optimum weights can therefore be pre-built with each set of the weights corresponding to a specific set of system parameters. During the mission, since the system parameters are measurable and controllable, the set of the optimum weights for the data to be processed can be simply called from a look-up table style library.

In this report we have further evaluated the performance of PSTAP using airborne radar data generated by the high fidelity airborne radar system simulation software, RLSTAP (Rome Laboratory Space-Time Adaptive Processing). We have also computed STAP results using the conventional diagonally loaded sample matrix inversion (DL-SMI) method. The STAP results serve as benchmarks to examine the results of PSTAP.

There are two ways of constructing the PSTAP optimum weights. One way is to use clutter models, which does not require either any specific knowledge of the clutter environment or any sample data. The second relies on test or previous flight data. A standard STAP procedure may be used to form the optimum weights using the test or previous flight data. Clutter environments of the test data and future data need not be the same or similar, but the radar and platform parameters are supposed to be the same in principle.

A total of nine datasets have been generated using the RLSTAP software. Clutter environments used in the simulation include the Seattle area and the Washington D.C. area. PSTAP results using weights constructed in both ways are compared to results of STAP. The comparison has shown that:

- PSTAP performs the same as or slightly better than STAP for all cases studied if optimum weights are constructed based on the clutter models.
- PSTAP performs the same as STAP for all cases studied if optimum weights are constructed using other data sets.

Most importantly, PSTAP builds a library of optimum weights a priori and therefore does not need computing computationally intensive optimum weights in real-time.

Author

Yunhan Dong

Electronic Warfare and Radar Division

Dr Yunhan Dong received his Bachelor and Master degrees in 1980s in China and his PhD in 1995 at UNSW, Australia, all in electrical engineering. He then worked at UNSW from 1995 to 2000, and Optus Telecommunications Inc from 2000 to 2002. He joined DSTO as a Senior Research Scientist in 2002. His research interests are primarily in radar signal and image processing, and radar backscatter modelling. Dr Dong was a recipient of both Postdoctoral Research Fellowships and Research Fellowships from the Australian Research Council.

Contents

1. INTRODUCTION	1
2. GENERATING DATASETS.....	2
3. SOME ISSUES.....	6
3.1 Clutter Foldover	6
3.2 Decorrelation	6
3.3 Sample Selection for STAP Covariance Matrix	9
3.4 Optimum Weights for PSTAP and STAP	9
4. RESULTS.....	10
4.1 Constructing Optimum Weights using Clutter Models	10
4.1.1 Results of Datasets #1, #2 and #3.....	10
4.1.2 Results of Datasets #4, #5 and #6.....	17
4.2 Constructing Optimum Weights using Other Flight Data	19
5. SUMMARY.....	23
6. ACKNOWLEDGEMENT	24
7. REFERENCES.....	24

1. Introduction

In scenarios where an airborne phased array Doppler radar is used in searching for moving targets whose signals are embedded in Gaussian distributed undesired signals including clutter (echoes from the terrain surface), noise jamming and thermal noise, space-time adaptive processing (STAP) provides the optimum signal-to-interference-and-noise ratio (SINR) (Ward, 1994, Klemm, 2002). However STAP normally requires the inverse of the covariance matrix (ICM) of undesired signals in order to form optimum weights to process received data. The typical dimension of the covariance matrix (CM) of undesired signals ranges from hundreds to thousands. It is this large computational load that prevents the implementation of fully adaptive STAP algorithms in most airborne radar systems at current computer speeds.

It has been proven that the ICM is approximately invariant to changes in clutter returns. Based on this we have proposed a pre-built space-time non-adaptive processor (PSTAP) in a previous DSTO Research Report (Dong, 2005). The approximate invariance of the ICM means that the ICM depends on radar system (radar and platform) parameters, but is approximately independent of the clutter environment. Optimum weights can therefore be pre-built, with each set of weights corresponding to a specific set of system parameters. During the mission, since system parameters are measurable and controllable, the set of optimum weights for the data to be processed can be simply called from a look-up table style library.

This report further evaluates the performance of PSTAP using airborne radar data generated by the high fidelity airborne radar system simulation software, Rome Laboratory Space-Time Adaptive Processing (RLSTAP). There are two ways of constructing PSTAP optimum weights. One is to use clutter models, which does not require either any specific knowledge of the clutter environment or any sample data. The second relies on test or previous flight data. A standard STAP procedure may be used to form the optimum weights using the test or previous flight data. Clutter environments of the test data and future data need not to be the same or similar, but the radar and platform parameters are supposed to be the same in principle.

The advantage of using clutter models to build optimum weights is that all possible combinations of radar and platform parameters can be presented in computation and the resultant optimum weights stored for later use. The problem is the fidelity of the models has to be verified for the specific system using the test flight data. Some effects may be difficult to model precisely. On the other hand, since the ICM is approximately invariant to the clutter environment, the optimum weights can also be constructed a priori simply using STAP procedures with test flight data. The advantage of this method is that there is no direct mathematical modelling involved in the construction of the weights. However, because the test flight data are limited, it is unlikely that the test data could cover all possible combinations of radar and platform parameters which may occur in the future missions. To reduce the number of possible combinations of radar and platform parameters, the pulse repetition frequency (PRF) can be linked to the platform velocity and to make the ratio of the two constant. This will be demonstrated in Section 4.

Results of PSTAP using both ways of constructing optimum weights are compared to results of STAP. The ICM for STAP is obtained using the conventional diagonally loaded sample matrix inversion (DL-SMI) method. On the other hand, PSTAP only requires radar and system parameters but does not require any sample data and any knowledge of the particular clutter environment to form the optimum weights if the construction is based on the clutter models. If the construction of the weights is based on the flight data, the difference between STAP and PSTAP is that the weights are obtained from and applied to the same dataset in former while the weights are obtained from one dataset and used to process another in latter.

2. Generating Datasets

A total of nine airborne radar datasets were generated by RLSTAP to support the assessment of PSTAP in this report. The first six datasets were mainly used to evaluate the performance of PSTAP in which the optimum weights were generated purely from modelling perspective. The last three datasets mainly served to evaluate the performance of PSTAP in which the optimum weights were generated from other datasets.

Datasets, #1, #2 and #3 were generated using the system and environmental parameters given in Table 1. All three datasets have the same radar and platform parameters as well as the same clutter environment. The only difference among them is the radar cross-section (RCS) of the targets. In particular, datasets #1, #2 and #3, respectively, contains three 10 m² targets, three 1 m² targets and three 0.1 m² targets. Table 2 lists parameters of these targets.

Datasets #4, #5 and #6 are similar to the first three datasets, except that

- The Washington D.C area was used as the clutter environment rather than the Seattle area;
- Platform height was 7 km rather than 10 km;
- Mainbeam was steered 30° from the broadside (east) rather than 0°.

Table 3 lists target parameters for datasets #4, #5 and #6.

Dataset #7 has the same parameters and clutter environment as dataset #5 except that the mainbeam was steered to the broadside.

Datasets #8 has all the same parameters and clutter environment as dataset #2 except that the platform speed was changed to 168.3 m/s.

Dataset #9 has all the same parameters and clutter environment as dataset #8 except that the PRF was changed to 1923 Hz. We will see the reasons for these changes in #8 and #9 later in the report.

For easy reference later in the report, the conditions under which these datasets were generated are summarised in Table 4.

Table 1: Parameters used in RLSTAP for generating first three airborne radar datasets.

Parameter	Specification
Radar	
Phased array	Linear 20-by-4 elements, element pattern $\cos^{0.6}(\phi)$, azimuth spacing 0.12m, elevation spacing 0.15m uniform tapering for transmit
Carrier frequency	1.2 GHz
Polarisation	VV
LFM bandwidth	2 MHz
PRF	2 kHz
Number of pulses per CPI	32
Peak power	30 kW
Duty	10%
Sample rate	0.2 μ s
Looking direction	Broadside (East), horizontal
Platform	
Height	10 km
Speed	175 m/s
Undesired signals	
Thermal noise	Gaussian
Clutter	Seattle area: (47.9°N, -123.9°E) to (47.0°N, -122.1°E)
Jamming	None

Table 2: Target parameters for the first three datasets.

Parameters	Target 1	Target 2	Target 3
Height (km)	5	5	5
Position off broadside direction	1 km North	0.5 km South	0
Radial velocity (m/s)	-75	-55	-65
Doppler frequency (Hz)	600	440	520
Range (km)	50	60	70
Range bin Number	1934	2266	2598
RCS (sqm)	10 / 1 / 0.1	10 / 1 / 0.1	10 / 1 / 0.1

Table 3: Target parameters for the second three datasets.

Parameters	Target 1	Target 2	Target 3
Height (km)	3	3	3
Position off mainlobe direction	1 km north	0.5 km south	0
Radial velocity (m/s)	-100	-20	150
Doppler frequency (Hz)	-500	860	-500
Range (km)	50	60	70
Range bin Number	1948	2256	2598
RCS (sqm)	10 / 1 / 0.1	10 / 1 / 0.1	10 / 1 / 0.1

Table 4: Datasets generated and used in the report.

Dataset	System Parameters	Clutter Environment	Target Parameters	Target RCS (sqm)
#1	Table 1	Seattle area	Table 2	10
#2	Ditto	Ditto	Ditto	1
#3	Ditto	Ditto	Ditto	0.1
#4	Table 1 except that the platform height is amended to 7 km and look angle to 30° from broadside.	Washington D.C. area	Table 3	10
#5	Ditto	Ditto	Ditto	1
#6	Ditto	Ditto	Ditto	0.1
#7	As #5 except that the look angle is to the broadside	Ditto	Ditto	1
#8	As #2 except the platform speed is changed to 168.3 m/s	Seattle area	Table 2 ¹	1
#9	As of #2 except the platform speed is changed to 168.3 m/s and the PRF to 1923 Hz	Ditto	Table 2 ²	1

RLSTAP calculates clutter returns based on the United States Geological Survey Land Use and Land Cover (USGS LULC) data and the Digital Terrain Elevation (DTE) data. The LULC data superposed onto the DTE data for the Seattle area and the Washington area, respectively, with the radar beam pattern, are shown in Figure 1 and Figure 2. Details of the clutter calculation model used in RLSTAP are unknown.

The unambiguous range is 75 km for the parameters given in Table 1. With the classical 4/3 Earth radius model, the range to the horizon is 412.5 km resulting in an up to five range foldovers. However due to the availability of the LCLU data, the simulation only took the first range foldover into the account. That is, clutter returns from beyond 150km

¹The Doppler frequencies of the targets change accordingly with the change in platform speed.

²See note 1.

were ignored. Because the clutter return decays as a function of the range to the third power, the effect of higher range foldovers is believed to be insignificant.

Before presenting results, it is worth discussing some issues that occurred in the processing.

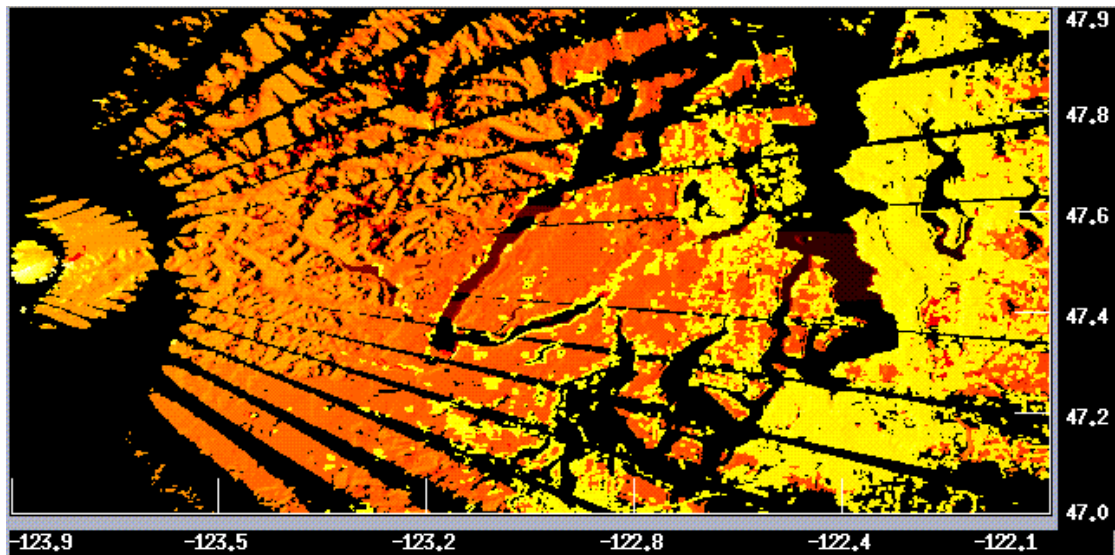


Figure 1: The LULC data superposed onto the DTE data of the Seattle area.

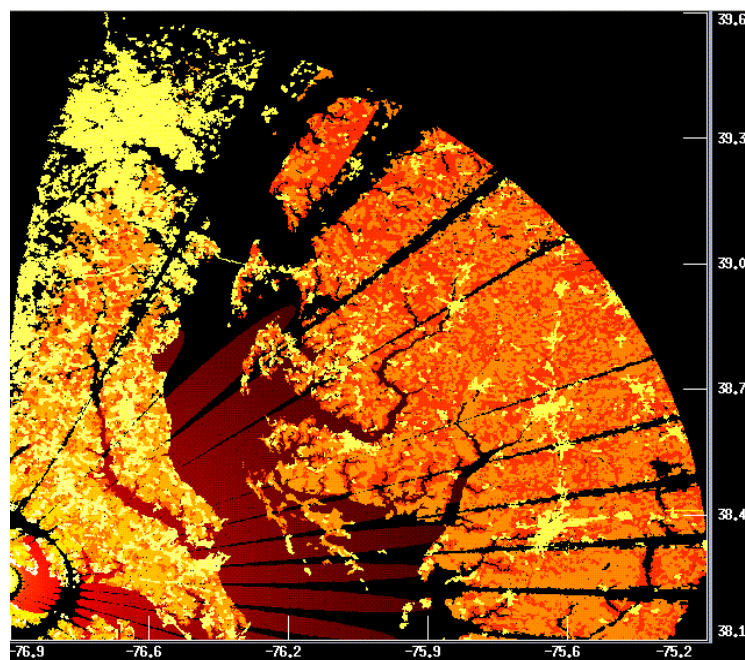


Figure 2: The LULC data superposed on the DTE data of the Washington D. C. area.

3. Some Issues

3.1 Clutter Foldover

For medium and high PRF radars, due to range ambiguity (clutter foldover), clutter returns received by the first few pulses are generally statistically different from the rest of the pulses in a CPI, unless the CPIs are continuous. This is because the data received by the first pulse contain no clutter foldover component, the data received by the second pulse contain the first clutter foldover component generated by the first pulse and so on. Some radars automatically discard the data collected by the first few pulses to make the received data statistically the same. The simulated RLSTAP data apparently “collected” all data generated by all pulses. Figure 3 shows three clutter profiles against range collected by receive element 1 for the first, second and third pulses, respectively. It can be seen that the data collected by pulse 1 and the data collected by pulse 2 or pulse 3 are statistically different, while the data collected by pulse 2 and pulse 3 are statistically the same. This is consistent with the given simulation conditions where the clutter return from the first clutter foldover was included (the rest of clutter foldovers were ignored due to the lack of the LULC data and DTE data for the extended area).

Therefore in our calculation only the data collected by the 2nd to 32nd pulses were used. Theoretically, the exclusion of the first pulse data results in a small coherent processing gain loss of $10\log_{10}(31/32) = -0.14\text{dB}$.

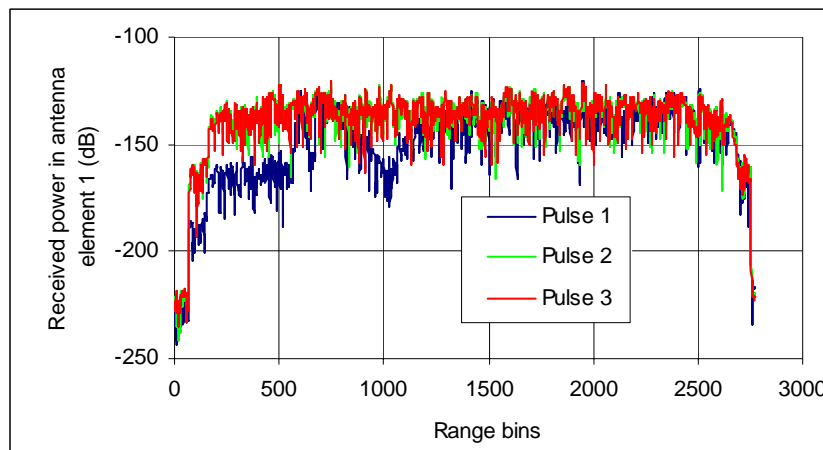
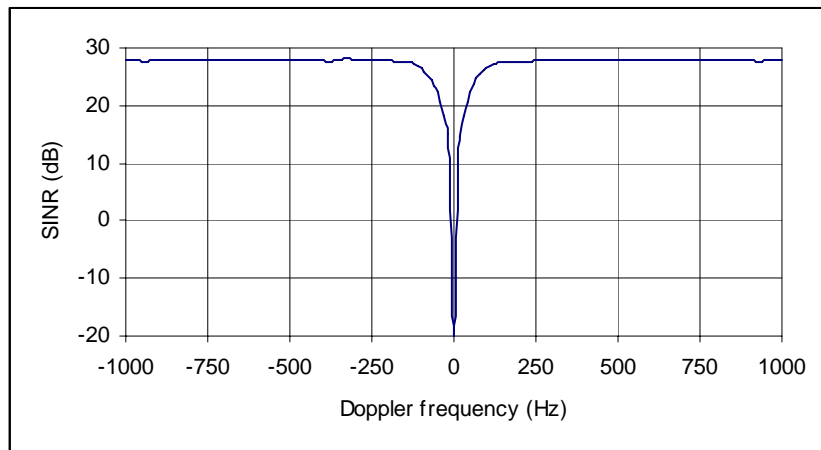


Figure 3: Three clutter profiles against range received by antenna element 1 for pulse 1, 2, and 3, respectively.

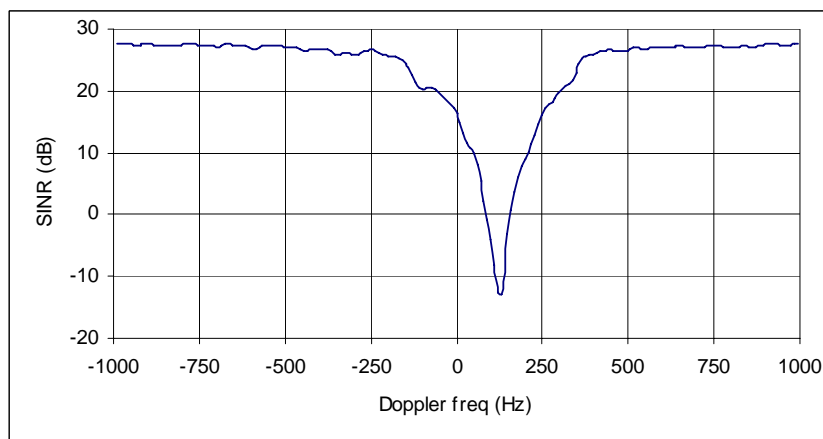
3.2 Decorrelation

In the analysis of real airborne radar data, Multi-Channel Airborne Radar Measurement (MCARM) data, it has been found that the most dominant decorrelation contributions

include range ambiguity and clutter intrinsic motion (Dong, 2005). The analysis of RLSTAP data however shows that only the contribution of range ambiguity is significant. The clutter notch of RLSTAP data is much narrower than that of MCARM data, although two radar systems have similar parameters. Figure 4 compares clutter notches of RLSTAP and MCARM data. The SINRs shown in the figure were computed using the STAP DL-SMI method. The shift of the notch of MCARM data is due to the crab angle of the aircraft. No crab angle was assumed in RLSTAP data.



(a) RLSTAP data



(b) MCARM data

Figure 4: Clutter notch comparison between (a) RLSTAP data and (b) MCARM data. The SINR curves are computed using the STAP DL-SMI method.

Spatial and temporal decorrelation due to clutter foldover, clutter intrinsic motion and platform motion usually broadens the SINR notch. Details of simulation models counting various decorrelation effects in RLSTAP are unknown. One possible explanation for the narrower notch of RLSTAP data may be the decorrelation models used in RLSTAP. Because the main purpose of this report is to evaluate the performance of PSTAP rather

than examining the fidelity of the simulation model, we will not further investigate this notch width difference. To best match the clutter notch, only the decorrelation effect due to range ambiguity is included in the PSTAP modelling for RLSTAP data. The decorrelation effect due to clutter intrinsic motion was not included, (ie, the clutter Doppler bandwidth was assumed to be 0 Hz). The comparison of the PSTAP SINR and the STAP SINR is shown in Figure 5. The level of the STAP SINR has been properly adjusted assuming that its maximum value approaches the theoretical maximum value. It can be seen, with the only range ambiguity effect taken into account, the notch width of the PSTAP SINR is almost identical to that of the STAP SINR. The loss of the PSTAP SINR, ie, the difference of the STAP SINR and the PSTAP SINR is shown in Figure 6. It can be seen that significant loss only occurs at the centre frequency of clutter, indicating that PSTAP should perform the same as STAP for detecting target signals whose Doppler frequencies differ from that of clutter. Furthermore the PSTAP can suppress clutter signal more than required because the notch of the PSTAP is deeper than that of the STAP.

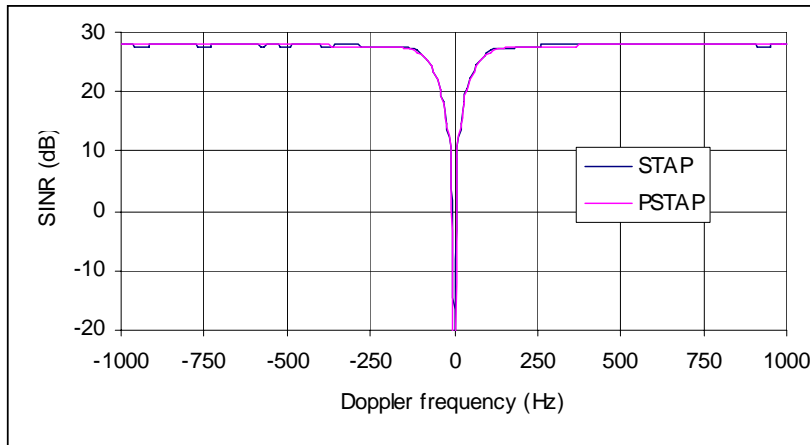


Figure 5: Comparison of the STAP SINR and the PSTAP SINR.

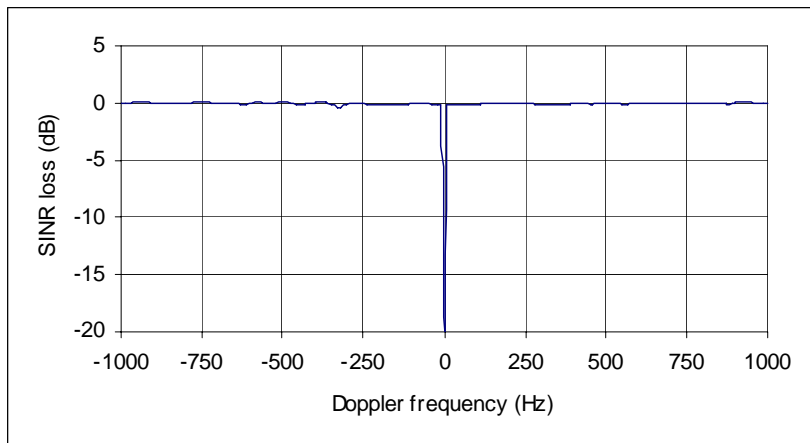


Figure 6: Loss of the PSTAP SINR compared to the STAP SINR. A significant loss only occurs at the centre frequency of clutter indicating that the PSTAP has a greater capability to suppress clutter than the STAP, while the target detection capabilities for both processors are about the same as the SINR loss elsewhere is close to zero dB.

3.3 Sample Selection for STAP Covariance Matrix

To compute the CM using the STAP DL-SMI method, one might think the more range samples the better. In fact this is not necessarily true because samples are generally not collected from a statistically homogenous clutter environment. Shown in Figure 7 is a comparison of sidelobe levels of target 1 in Dataset #2 (1m² RCS, at range bin 1934) detected by the STAP DL-SMI method with different selections of range samples for the CM. In particular the sample range bins for the four cases shown in the figure are:

- Case 1: range bins 800-2650 with the exclusion of target range bins themselves (the target range bins for targets 1, 2 and 3 are 1934, 2266 and 2598, respectively) as well as 10 nearest range bins on both sides of each target range bin;
- Case 2: range bins 1634-2234 with the exclusion of 1924-1944 (the target range bin is 1934)
- Case 3: range bins 800-1600 (no target in this region);
- Case 4: range bins 1000-1600 (no target in this region).

It can be seen from the figure that case 1 has the worst sidelobe level, although the greatest number of range samples were used. Sidelobe levels of the other three cases are about the same. In this report, case 4 was used to compute the CM in the DL-SMI method to obtain STAP results.

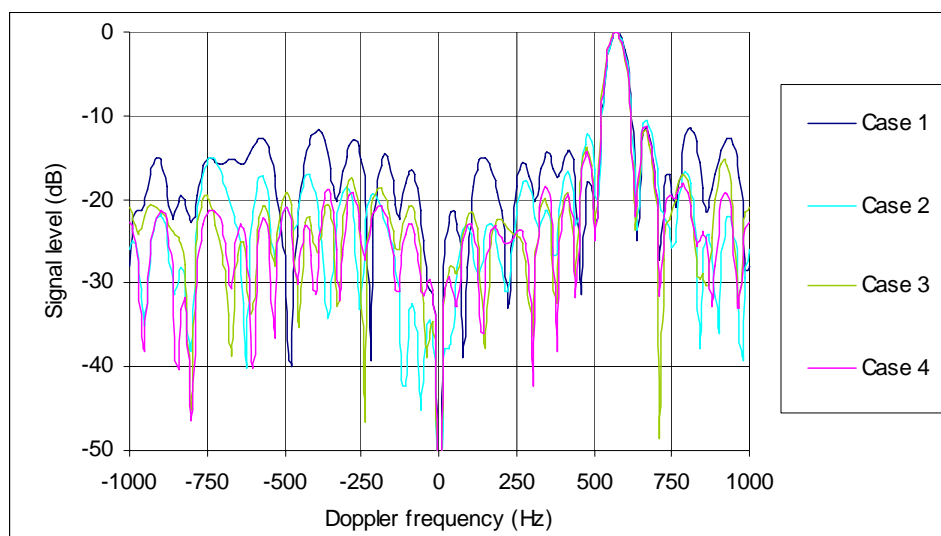


Figure 7: Sidelobe level comparison using the covariance matrices computed from different sample regions. Case 1 has the worst sidelobe level.

3.4 Optimum Weights for PSTAP and STAP

Construction of PSTAP optimum weights requires knowledge of the radar's elevation angle relative to the terrain surface for a given range. Since the elevation angle of the terrain differs from range bin to range bin, theoretically each range bin should require a set

of optimum weights. However, it has been shown in the previous report that the ICM is robust and not very sensitive to variations in elevation angle (Dong, 2005). For range bins 1700-2650 (wide enough to cover all targets), the corresponding elevation angle varies from 13.46° to 8.04° . It is believed that for such a variation in elevation angle, the differences among the ICMs should be insignificant. Therefore, only one single set of weights corresponding to range bin 2715 (the central range bin of 1700-2650) was constructed for PSTAP. This single set of the optimum weights was used in PSTAP to process all range bins 1700-2650. That the ICM not sensitive to the variations in elevation angle has also been observed in the STAP DL-SMI method as shown in Figure 7 where the results of cases 2 to 4 are about the same although the number of samples as well as the sections of samples selected are different. Similarly, therefore, only a single CM computed from range bins 1000-1600 was used to process data in range bins 1700-2650 in STAP.

4. Results

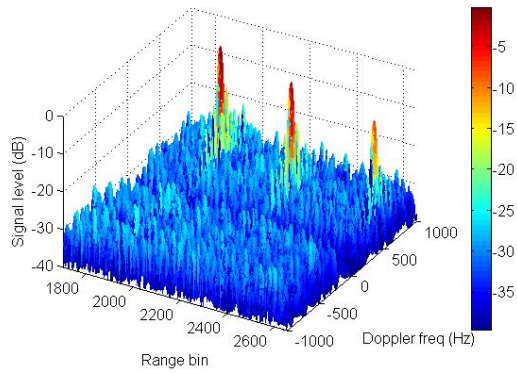
As indicated that there are two ways of constructing optimum weights for PSTAP: (1) by modelling and (2) based on other flight data. Results of these two ways are presented in Subsections 4.1 and 4.2, respectively. Meanwhile results of STAP are also presented as benchmarks to evaluate the performance of PSTAP.

4.1 Constructing Optimum Weights using Clutter Models

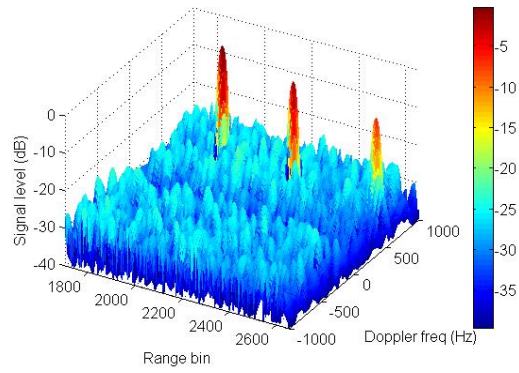
In this subsection PSTAP optimum weights were constructed from the clutter models (Dong, 2005), which requires neither any knowledge of specific clutter environments nor any sample data.

4.1.1 Results of Datasets #1, #2 and #3

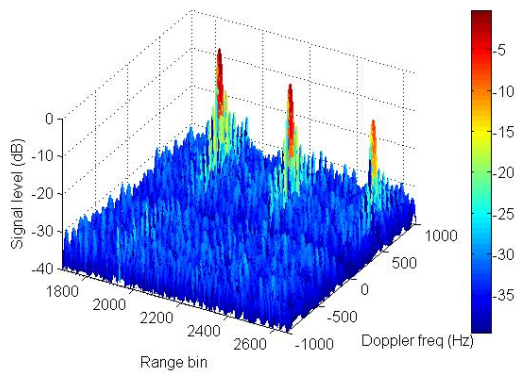
Results of target detection applying STAP and PSTAP to Datasets #1, #2 and #3 are shown in Figure 8 to Figure 10, where range bins 1700-2650 have been processed to include all three targets. Each figure shows four results, two comparing STAP and PSTAP without use of any window function, and the other two with use of the hamming window function (the window function was used in both the temporal and spatial domains). As anticipated, with the use of the hamming window function, sidelobe levels become lower and noise spikes are smoothed, but the resolution also becomes poorer. Two-dimensional plots for the range bins containing targets without use of any window function are shown in Figure 11 to Figure 13. Overall both STAP and PSTAP perform approximately the same, with the latter exhibiting slightly lower sidelobes. It has also been observed that for the scenario of 0.1 m^2 targets, the first two targets are only marginally detectable if not totally non-detectable, while the third seems to become totally non-detectable, as it is further away from the radar.



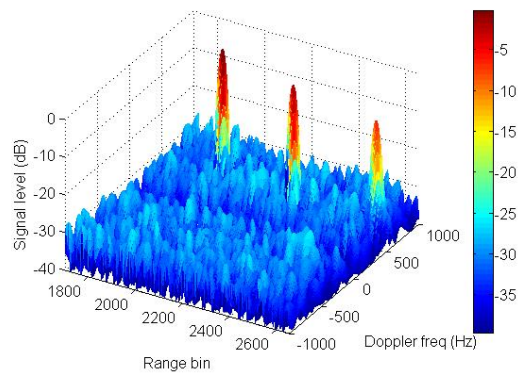
(a) STAP with uniform window



(b) STAP with Hamming window

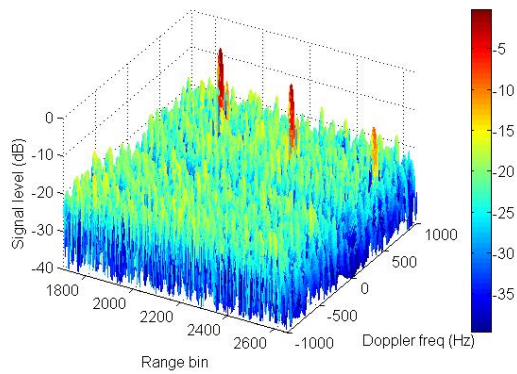


(c) PSTAP with uniform window

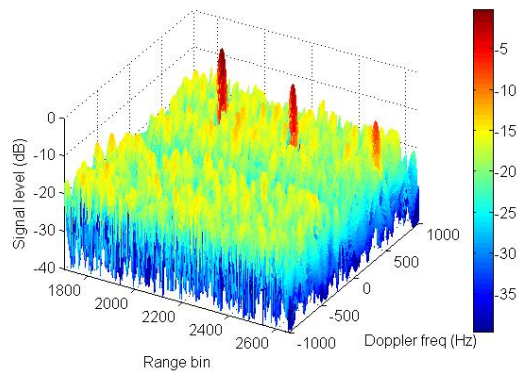


(d) PSTAP with Hamming window

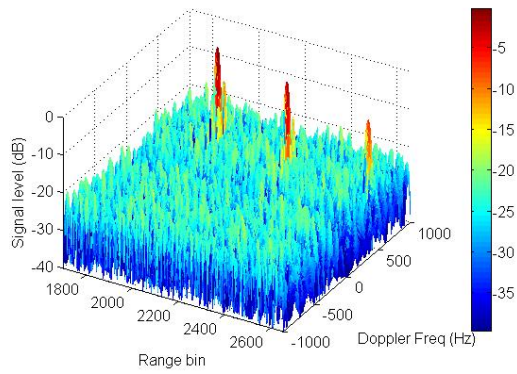
Figure 8: Comparison of STAP and PSTAP for detecting targets of $10m^2$ RCS in Dataset #1.



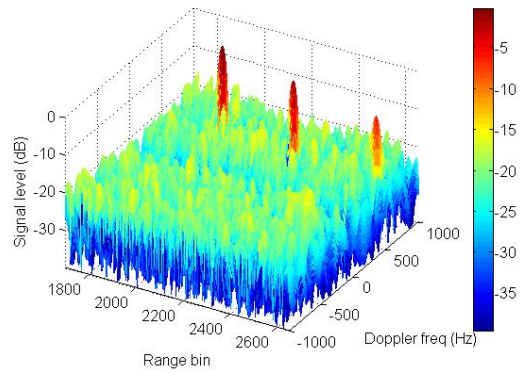
(a) STAP with uniform window



(b) STAP with Hamming window

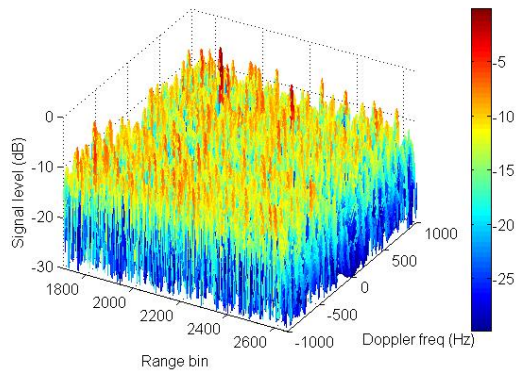


(c) PSTAP with uniform window

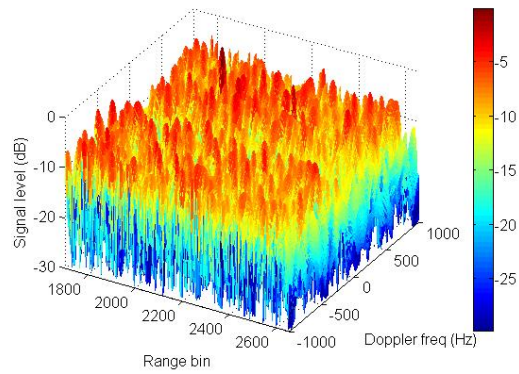


(d) PSTAP with Hamming window

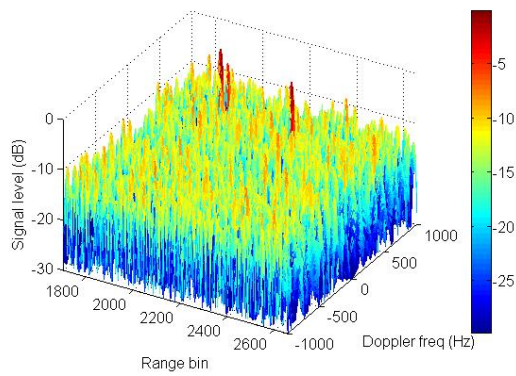
Figure 9: Comparison of STAP and PSTAP for detecting targets of $1m^2$ RCS in Dataset #2.



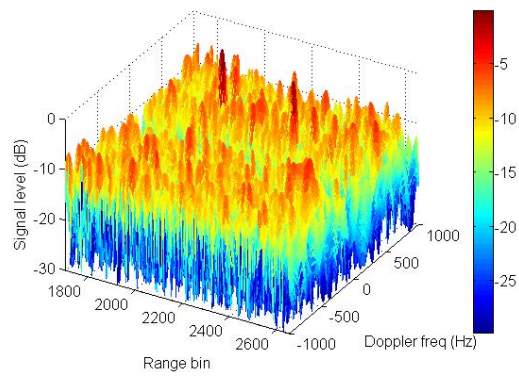
(a) STAP with uniform window



(b) STAP with Hamming window

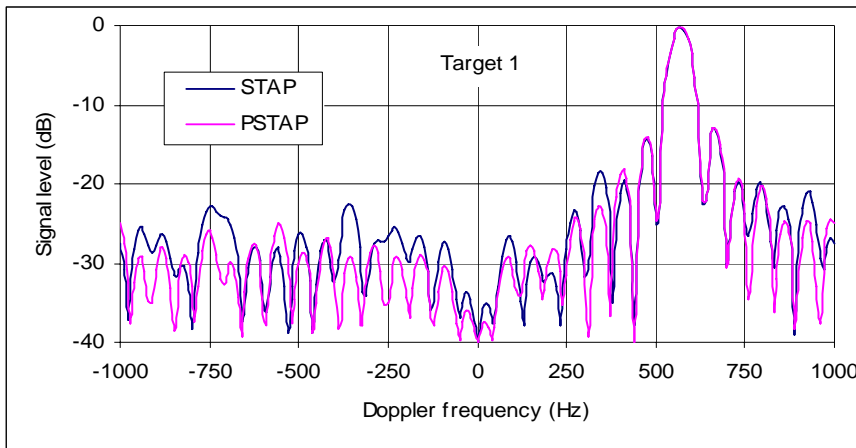


(c) PSTAP with uniform window

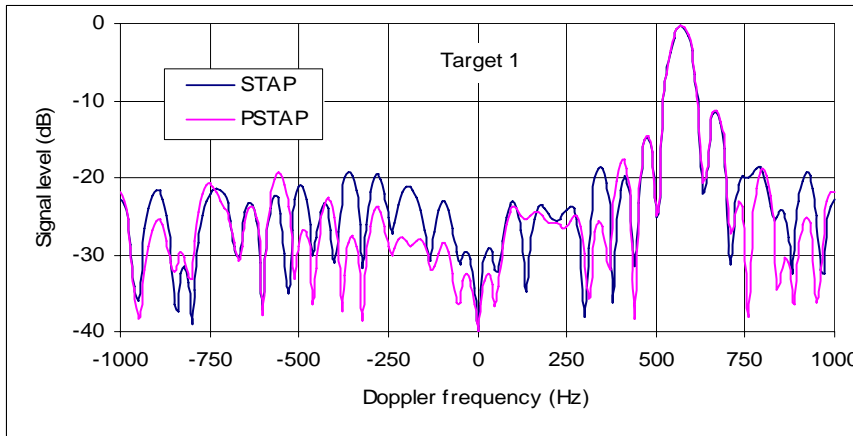


(d) PSTAP with Hamming window

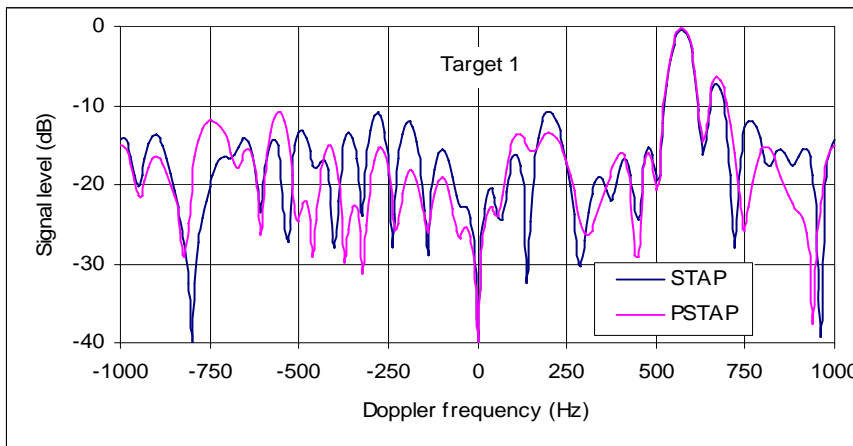
Figure 10: Comparison of STAP and PSTAP for detecting targets of $0.1m^2$ RCS in Dataset #3.



(a) 10 m² target in Dataset #1

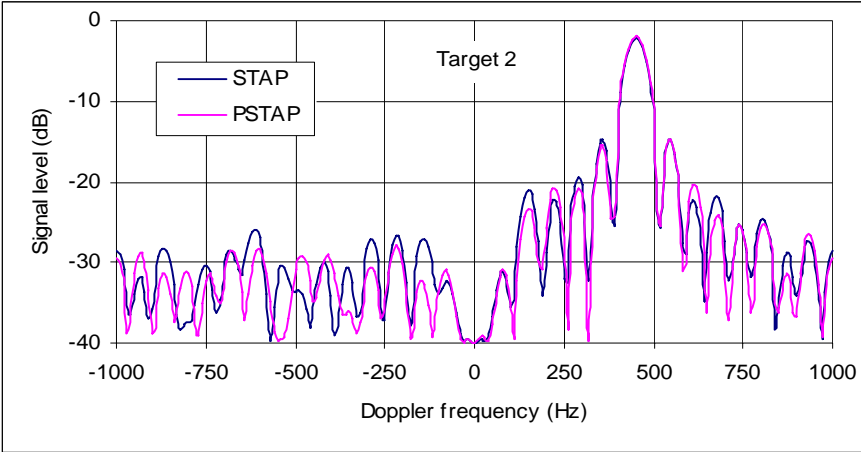


(b) 1 m² target in Dataset #2

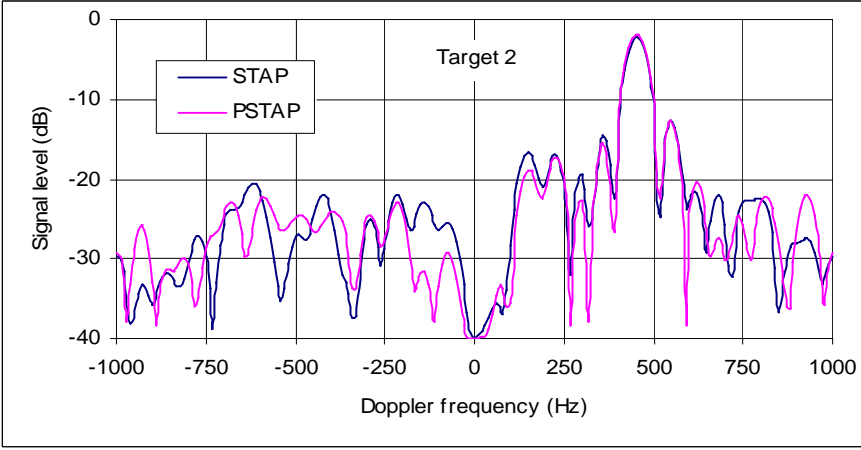


(c) 0.1 m² target in Dataset #3

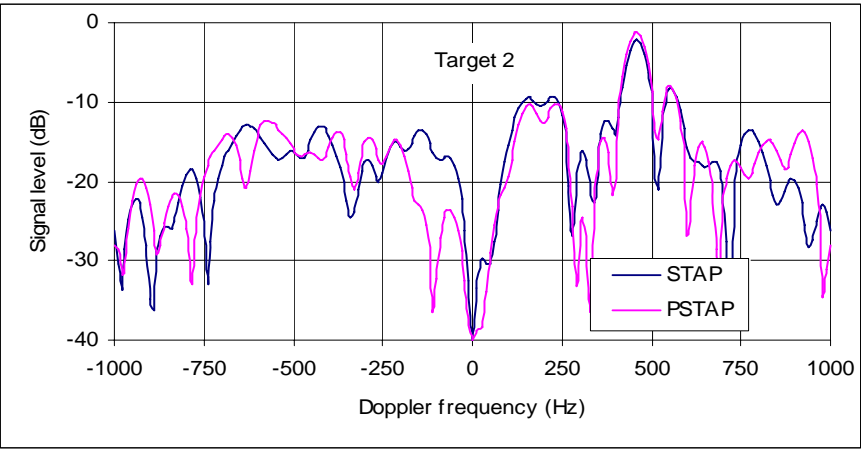
Figure 11: Sidelobe comparison between STAP and PSTAP for target 1 in Datasets #1, #2, and #3.



(a) 10 m² target in Dataset #1

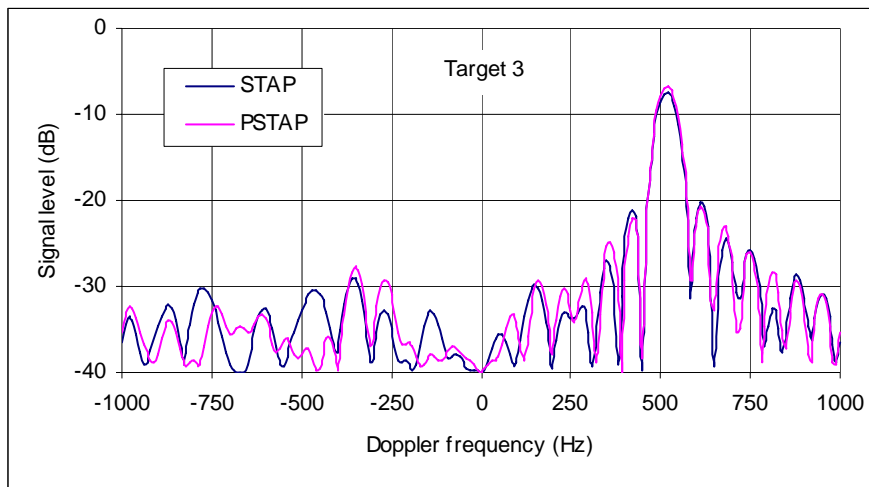


(b) 1 m² target in Dataset #2

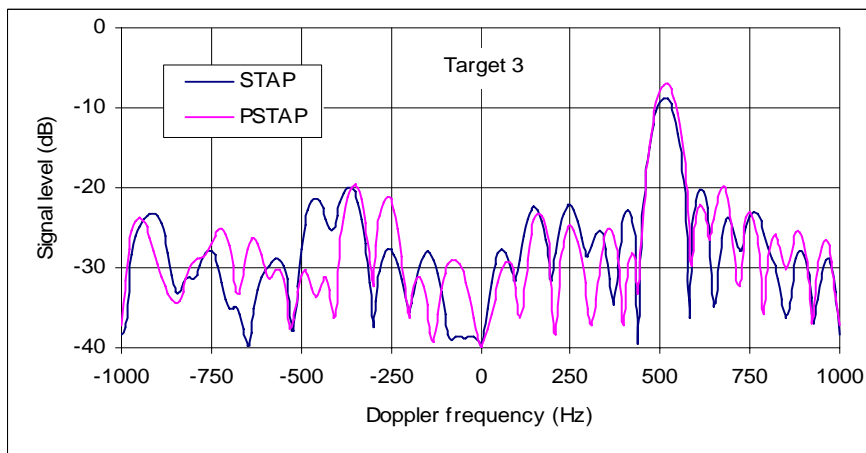


(c) 0.1 m² target in Dataset #3

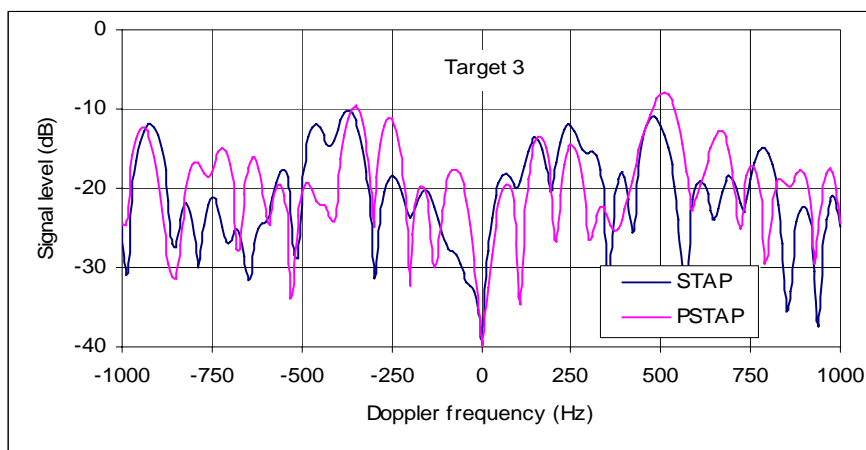
Figure 12: Sidelobe comparison between STAP and PSTAP for target 2 in Datasets #1, #2 and #3.



(a) 10 m² target in Dataset #1



(b) 1 m² target in Dataset #2



(c) 0.1 m² target in Dataset #3

Figure 13: Sidelobe comparison between STAP and PSTAP for target 3 in Datasets #1, #2 and #3.

4.1.2 Results of Datasets #4, #5 and #6

Results of target detection applying STAP and PSTAP to Datasets #4, #5 and #6 are shown in Figure 14 to Figure 16. Because the beam was steered 30° from the broadside, the clutter notch is shifted from 0 Hz and close to the frequency of the target 2. The results and conclusions are similar to those presented in Subsection 4.1.1. That is, both STAP and PSTAP perform approximately the same, with the latter having slightly lower sidelobes.

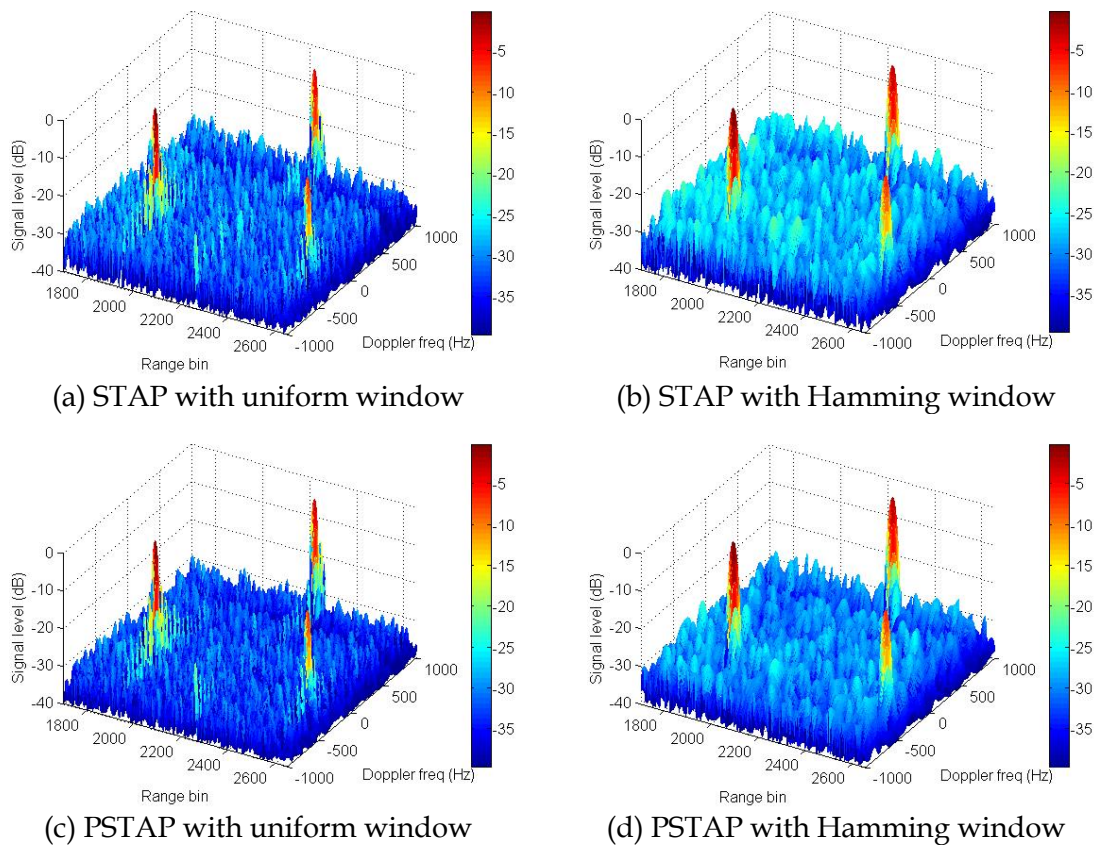
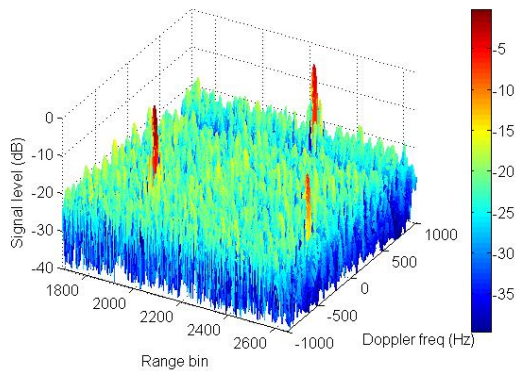
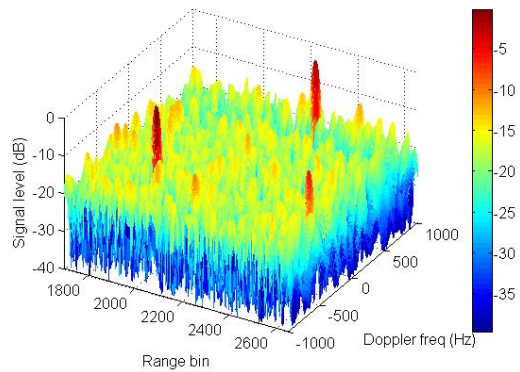


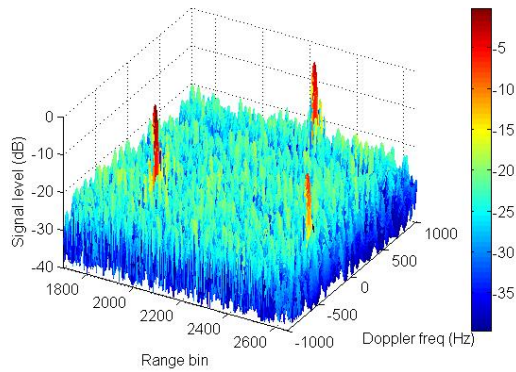
Figure 14: Comparison between STAP and PSTAP for detecting 10m^2 targets in Dataset #4.



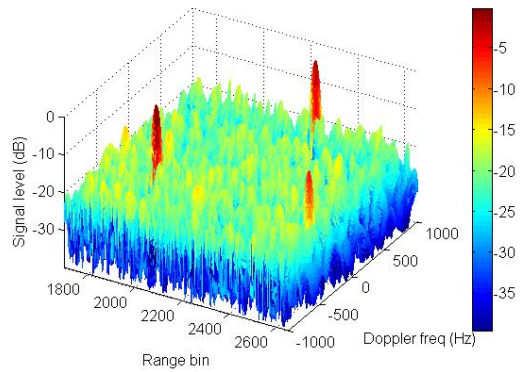
(a) STAP with uniform window



(b) STAP with Hamming window



(c) PSTAP with uniform window



(d) PSTAP with Hamming window

Figure 15: Comparison between STAP and PSTAP for detecting $1m^2$ targets in Dataset #5.

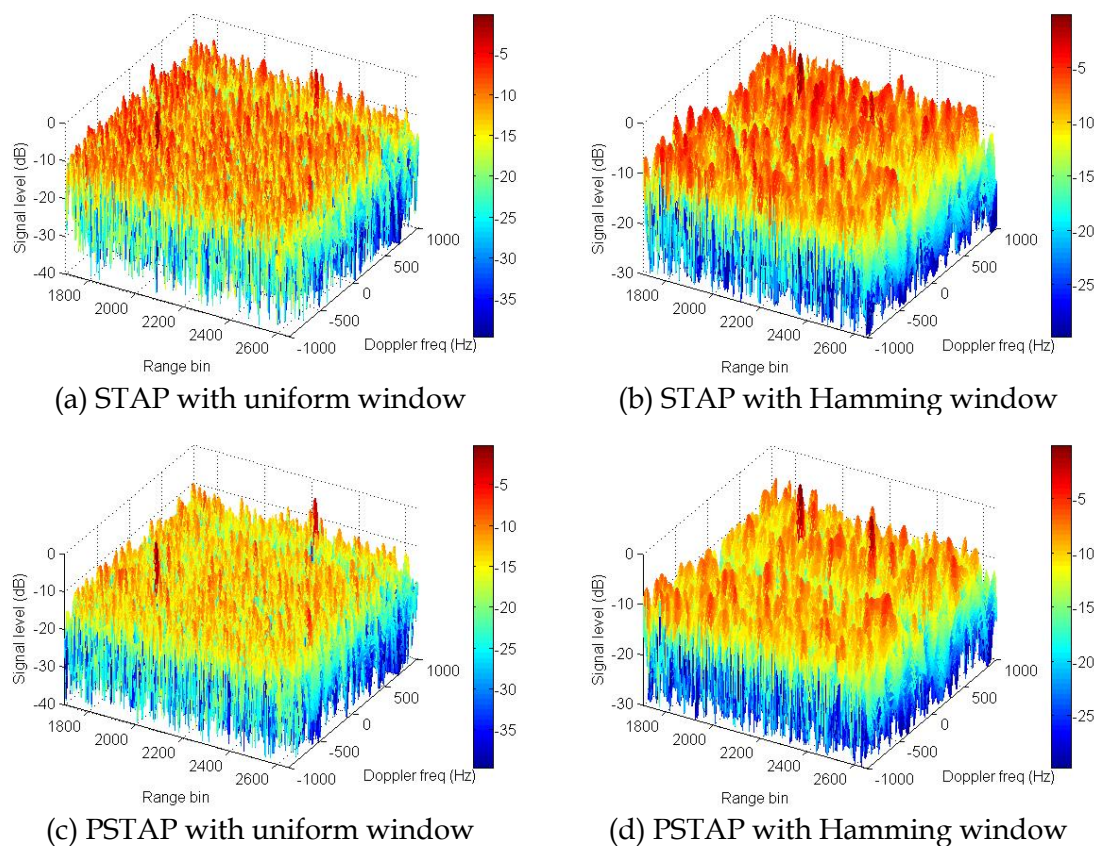


Figure 16: Comparison between STAP and PSTAP for detecting 0.1 m^2 targets in Dataset #6.

4.2 Constructing Optimum Weights using Other Flight Data

Instead of using modelling procedure, PSTAP optimum weights can also be formed using data collected by other flight data. Because the ICM is approximately invariant to clutter returns, the ICM or weights of PSTAP can be computed from other datasets using a STAP method such as the conventional DL-SMI method. This pre-computed ICM or weights can then be directly applied to datasets collected in the future, provided that the radar and platform parameters, including the configuration of the phased array, frequency, polarisation, waveform, PRF, coherent processing interval (CPI), and platform speed etc, for these datasets are the same. In this way, there is no need to compute the ICM or weights in real-time.

For convenience we bracket a pair of datasets together to indicate that the first dataset in the brackets is used to form the optimum weights which are then applied to the second dataset for target detection. For instance ($\#x, \#y$) means that the weights are generated from Dataset $\#x$ and applied to Dataset $\#y$ for target detection.

Datasets #2 and #7 were first used for the study. According to Table 4, all parameters for these two datasets are the same except:

- Dataset #2 used the Seattle area as the clutter environment with a platform height of 10km;
- Dataset #7 used the Washington D.C. area as the clutter environment with a platform height of 7km.

The results are shown in Figure 17 and Figure 18. Each figure shows the result of STAP (#x and #y are the same) as well as the result of PSTAP (#x and #y are different). Interestingly, Figure 17 shows that PSTAP performs slightly better (lower sidelobes), while the opposite is found in Figure 18.

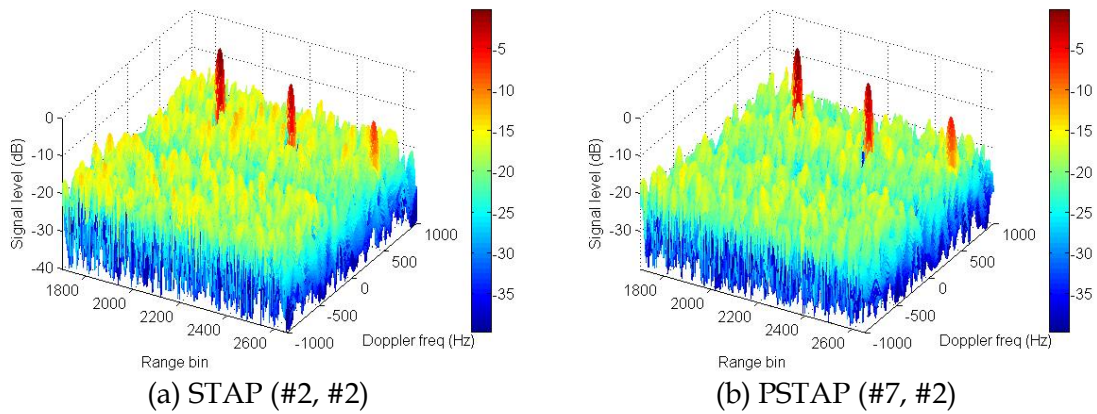


Figure 17: Comparison between STAP and PSTAP for detecting 1 m^2 targets in Date set #2. PSTAP uses the ICM computed from Dataset #7.

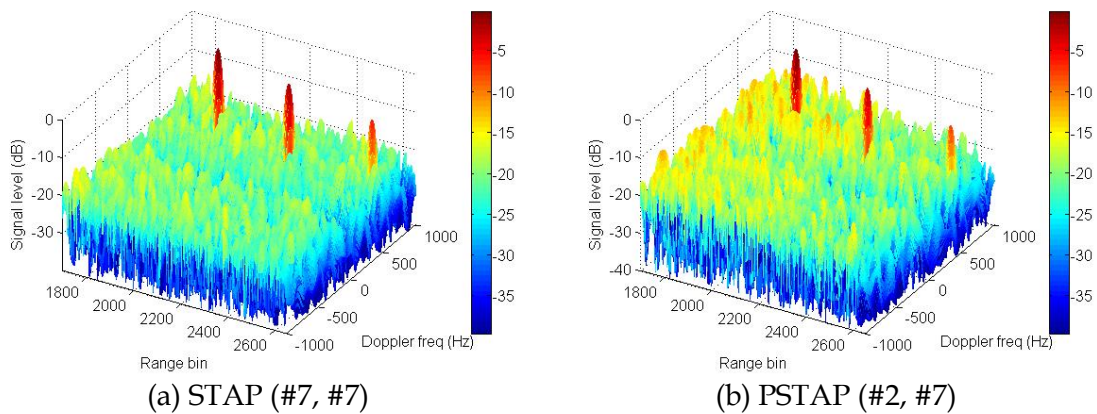


Figure 18: Comparison between STAP and PSTAP for detecting 1 m^2 targets in Dataset #7. PSTAP uses the ICM computed from Dataset #2.

We have indicated and demonstrated that the radar and platform parameters (except the height of the platform) should be the same if PSTAP weights are obtained from other flight data. Let us now examine the effects of changing platform speed on PSTAP weights. All the parameters including the clutter environment are the same for Datasets #2 and #8 except the platform speed which is 175 m/s for the former and 168.3 m/s for the latter. The results of STAP and PSTAP are shown in Figure 19 (a) and (b), respectively. It can be seen that the PSTAP result degrades significantly compared to the STAP result, due to the platform speed difference (about 4%) between the two datasets.

A similar result is shown in Figure 19 (c) where the weights were generated from Dataset #7 and applied to Dataset #8. The differences between Datasets #7 and #8 include the platform speed and the clutter environment.

Figure 19 (d) shows another PSTAP result, in which the weights were generated from Dataset #9 and applied to Dataset #8. All parameters including platform speed and the clutter environment are the same for Datasets #8 and #9 except the PRF which is 2000 Hz for the former and 1923 Hz for the latter.

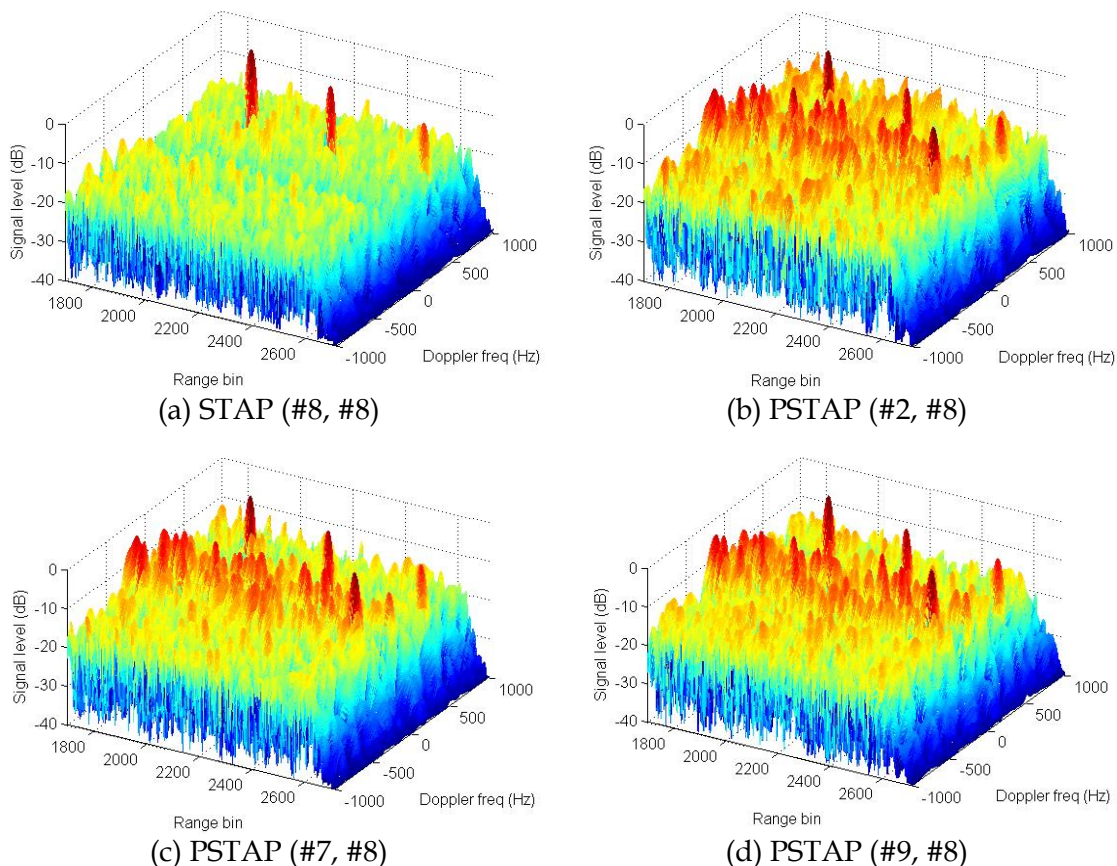


Figure 19: PSTAP does not work, if the system parameters in the dataset used to construct the weights are different from parameters in the dataset being processed.

It is observed from the examples shown in Figure 19 (b), (c) and (d) that PSTAP cannot perform at the same level as STAP if the platform speed or PRF is different between the dataset used to generate the weights and the dataset being processed, though the other radar and platform parameters may remain the same. In the space-time steering vector, the platform speed v_a and the PRF f_r are linked to the ratio of the normalised Doppler frequency to the normalised spatial frequency, β through (Ward, 1994),

$$\beta = 2 \frac{v_a}{f_r d} \quad (1)$$

where d is the antenna element interval.

It has been predicted in the previous report (Dong, 2005) that if β is constant and the other radar and platform parameters remain the same, PSTAP should be unaffected by changes in v_a and f_r . To examine this prediction, two PSTAP results are compared to the STAP results for Dataset #9 as shown in Figure 20. For the PSTAP results shown in Figure 20 (b) and (c), the weights were generated from Datasets #2 and #7, respectively. Datasets #2 and #9 were generated with the same clutter environment of the Seattle area, and the ratio of v_a / f_r is $175/2000 = 0.0875$ for #2 and $168.3/1923 = 0.0875$ for #9. Dataset #7 has the same values of v_a and f_r as #2, but with a different clutter environment (Washington D.C area). Another difference between #7 and #9 is the platform height which is 7 km for the former and 10 km for the latter. It can be seen as long as the ratio of v_a / f_r is the same for the dataset used to generate the weights and the dataset being processed, PSTAP is still able to perform the same as STAP.

From the above comparisons, we observe that:

- The approximate invariance of the ICM allows optimum weights to be pre-built based on other flight data using a STAP method such as the DL-SMI method.
- The pre-built optimum weights can generally only be used to process data collected with the same radar and platform parameters. However, as the ICM is not very sensitive to grazing angle, the platform height in the dataset used to form optimum weights and in the datasets to be processed can be different. Two datasets with platform heights 7 km and 10 km, respectively, have been mutually used to form the optimum weights and process the other dataset and no performance deterioration has been found.
- The pre-built optimum weights can be used to process data collected with different platform speeds as long as the ratio of the platform speed to the PRF maintains constant.
- In general PSTAP performs the same as STAP for most cases studied. However for a particular case, it may perform better or worse. Figure 17 shows that PSTAP has lower sidelobes than STAP, while Figure 18 illustrates the opposite. The reason is still under investigation.

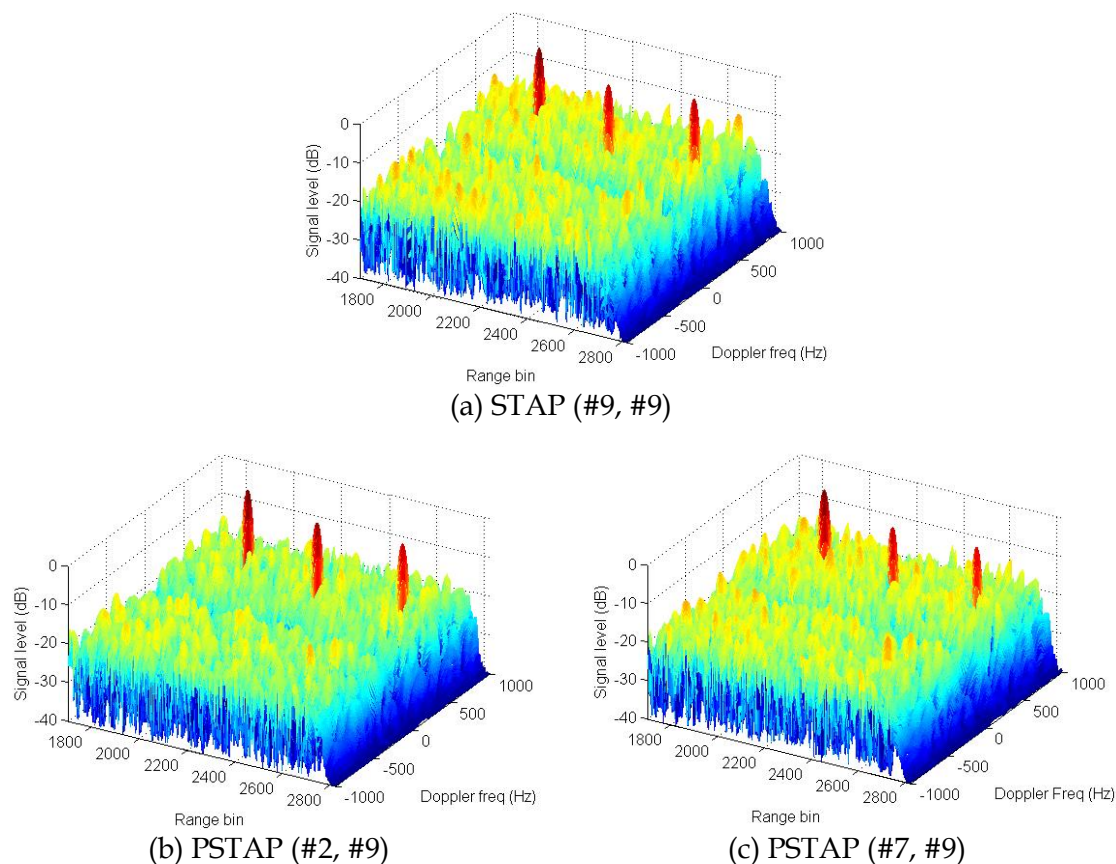


Figure 20: PSTAP still works, if the dataset used to construct the weights and the dataset to be processed have the same ratio of v_a / f_r .

5. Summary

To process airborne phased array Doppler radar data, STAP (space-time adaptive processing) provides the optimum SINR (signal-to-interference-and-noise ratio) in detecting target signals embedded in undesired signals including clutter, jamming and thermal noise. The bottleneck that prevents the fully adaptive STAP from implementation in real-time radar systems is the time requirement for computing the ICM (the inverse of the covariance matrix) to construct optimum weights.

For a side-looking scenario, we have proven that the ICM is approximately invariant to changes in the clutter returns (Dong, 2005). Based upon this, we have proposed PSTAP (pre-built space-time non-adaptive processing). Optimum weights can be pre-built without knowing the clutter environment to significantly reduce real-time computational demand. We have successfully applied PSTAP to MCARM (Multi-Channel Airborne

Radar Measurement) data and shown that PSTAP performs the virtually same as STAP in a previous report (Dong 2005).

This report has further applied PSTAP to data generated by the high fidelity airborne radar simulation software, RLSTAP (Rome Laboratory Space-Time Adaptive Processing). Results calculated from the STAP DL-SMI (diagonally loaded sample matrix inversion) method have been used as benchmarks to evaluate the performance of PSTAP.

Using PSTAP, the pre-built optimum weights can be constructed through two ways. One is based on clutter models and the other relies on the test flight data. The advantage of the former is that any combinations of the system parameters can be selected in calculation so a library of optimum weights can be easily constructed. The advantage of the latter is that optimum weights can be computed from the test or previous flight data applying the usual STAP procedures. In this way, some difficult modelling issues can be avoided. The problem of the latter, however, is that it seems impossible to have test flight data cover all combinations of system parameters which are likely encountered in the future missions. If the PRF (pulse repetition frequency) is linked to the platform speed, then the number of possible combinations of the radar and system parameters can be greatly reduced.

A total of nine datasets have been generated using RLSTAP. Clutter environments in the simulation include the Seattle and the Washington D.C. areas. PSTAP results using the weights constructed in both ways are compared to STAP results. The comparison indicates that

- PSTAP performs the same as or slightly better than the STAP for all cases studied if optimum weights are constructed based on the clutter models.
- PSTAP performs the same as the STAP for all cases studied if the weights are constructed using other datasets.

6. Acknowledgement

The author sincerely thanks Mr A Mahoney for generating all airborne radar datasets using RLSTAP for this report. The Air Force Research Laboratory (AFRL) provided the RLSTAP software. Dr J Whitrow read the first draft of the report, and provided useful comments.

7. References

Dong, Y (2005) Approximate invariance of the inverse of the covariance matrix and the resultant pre-built STAP processor, Research Report, DSTO-RR-0291, DSTO.

Klemm, R (2002) *Principles of space-time adaptive processing*, 2nd edition, IEE.

Ward, J (1994) Space-time adaptive processing for airborne radar, Technical Report, TR-1015, Lincoln Laboratory, MIT.

DISTRIBUTION LIST
Evaluation of Pre-built Space-Time Non-Adaptive Processing (PSTAP)

Yunhan Dong

AUSTRALIA

DEFENCE ORGANISATION	No. of copies
Task Sponsor, OCAEWCSPO	1
S&T Program	
Chief Defence Scientist	} 1 Shared Copy
FAS Science Policy	
AS Science Corporate Management	
Director General Science Policy Development	
Counsellor Defence Science, London	Doc Data Sheet
Counsellor Defence Science, Washington	Doc Data Sheet
Scientific Adviser to MRDC, Thailand	Doc Data Sheet
Scientific Adviser Joint	1
Navy Scientific Adviser	Doc Data Sheet & Dist List
Scientific Adviser – Army	Doc Data Sheet & Dist List
AirForce Scientific Adviser	1
Scientific Adviser to the DMO	1
Systems Sciences Laboratory	
Chief of EWRD	Doc Data Sht & Dist List
Research Leader Microwave Radar	Doc Data Sht & Dist List
Head RST, EWRD: Dr J Whitrow	1
Task Manager: Mr G Lawrie	1
Head IRS, ISRD: Dr N Stacy	1
Head RFS, WSD: Dr A Szabo	1
Mr S Capon, RST Group, EWRD	1
Dr J Fabrizio, ISRD	1
Dr P Berry RMA Group, EWRD	1
Dr M Southcott, EWRD, AEW&C Resident Project Team (Baltimore)	1
Author: Dr Y Dong, EWRD	1
EWSTIS	1 PDF
DSTO Library and Archives	
Library Edinburgh	1
Defence Archives	1
Capability Development Group	
Director General Maritime Development	Doc Data Sheet
Director General Land Development	1
Director General Integrated Capability Development	1
Director General Capability and Plans	Doc Data Sheet
Assistant Secretary Investment Analysis	Doc Data Sheet
Director Capability Plans and Programming	Doc Data Sheet

Director General Australian Defence Simulation Office	Doc Data Sheet
Chief Information Officer Group	
Director General Australian Defence Simulation Office	Doc Data Sheet
Director General Information Policy and Plans	Doc Data Sheet
AS Information Strategy and Futures	Doc Data Sheet
AS Information Architecture and Management	Doc Data Sheet
Director General Information Services	Doc Data Sheet
Strategy Group	
Director General Military Strategy	Doc Data Sheet
Assistant Secretary Strategic Policy	Doc Data Sheet
Assistant Secretary Governance and Counter-Proliferation	Doc Data Sheet
Navy	
Maritime Operational Analysis Centre, Building 89/90 Garden Island Sydney NSW Deputy Director (Operations) Deputy Director (Analysis)	Doc Data Sht & Dist List
Director General Navy Capability, Performance and Plans, Navy Headquarters	Doc Data Sheet
Director General Navy Strategic Policy and Futures, Navy Headquarters	Doc Data Sheet
Air Force	
SO (Science) - Headquarters Air Combat Group, RAAF Base, Williamtown NSW 2314	Doc Data Sht & Exec Summ
Army	
ABCA National Standardisation Officer Land Warfare Development Sector, Puckapunyal	e-mailed Doc Data Sheet
SO (Science) - Land Headquarters (LHQ), Victoria Barracks NSW	Doc Data Sht & Exec Summ
SO (Science), Deployable Joint Force Headquarters (DJFHQ) (L), Enoggera QLD	Doc Data Sheet
Joint Operations Command	
Director General Joint Operations	Doc Data Sheet
Chief of Staff Headquarters Joint Operations Command	Doc Data Sheet
Commandant ADF Warfare Centre	Doc Data Sheet
Director General Strategic Logistics	Doc Data Sheet
COS Australian Defence College	Doc Data Sheet
Intelligence and Security Group	
AS Concepts, Capability and Resources	1
DGSTA , DIO	1
Manager, Information Centre, Defence Intelligence Organisation	1 (PDF)
Assistant Secretary Capability Provisioning	Doc Data Sheet
Assistant Secretary Capability and Systems	Doc Data Sheet

Defence Materiel Organisation

Deputy CEO	Doc Data Sheet
Head Aerospace Systems Division	Doc Data Sheet
Head Maritime Systems Division	Doc Data Sheet
Head Electronic and Weapon Systems Division	Doc Data Sheet
Program Manager Air Warfare Destroyer	Doc Data Sheet

Defence Libraries

Library Manager, DLS-Canberra	Doc Data Sheet
-------------------------------	----------------

OTHER ORGANISATIONS

National Library of Australia	1
NASA (Canberra)	1
Library of New South Wales	1
State Library of South Australia	1

UNIVERSITIES AND COLLEGES

Australian Defence Force Academy

Library	1
Head of Aerospace and Mechanical Engineering	1
Serials Section (M list), Deakin University Library, Geelong, VIC	1
Hargrave Library, Monash University	Doc Data Sheet
Librarian, Flinders University	1

OUTSIDE AUSTRALIA

INTERNATIONAL DEFENCE INFORMATION CENTRES

US Defense Technical Information Center	1 PDF
UK Dstl Knowledge Services	1 PDF
Canada Defence Research Directorate R&D Knowledge & Information Management (DRDKIM)	1
NZ Defence Information Centre	1

ABSTRACTING AND INFORMATION ORGANISATIONS

Library, Chemical Abstracts Reference Service	1
Engineering Societies Library, US	1
Materials Information, Cambridge Scientific Abstracts, US	1
Documents Librarian, The Center for Research Libraries, US	1

INFORMATION EXCHANGE AGREEMENT PARTNERS

National Aerospace Laboratory, Japan	1
National Aerospace Laboratory, Netherlands	1

SPARES	5
--------	---

Total number of copies: 45 Printed: 41 PDF: 4

DEFENCE SCIENCE AND TECHNOLOGY ORGANISATION DOCUMENT CONTROL DATA				1. PRIVACY MARKING/CAVEAT (OF DOCUMENT)	
2. TITLE Evaluation of Pre-Built Space-Time Non-Adaptive Processing (PSTAP)			3. SECURITY CLASSIFICATION (FOR UNCLASSIFIED REPORTS THAT ARE LIMITED RELEASE USE (L) NEXT TO DOCUMENT CLASSIFICATION) Document (U) Title (U) Abstract (U)		
4. AUTHOR(S) Yunhan Dong			5. CORPORATE AUTHOR Defence Science and Technology Organisation PO Box 1500 Edinburgh South Australia 5111 Australia		
6a. DSTO NUMBER DSTO-RR-0295		6b. AR NUMBER AR-013-463		6c. TYPE OF REPORT Research Report	7. DOCUMENT DATE July 2005
8. FILE NUMBER 2005/1059963	9. TASK NUMBER AIR 02/232	10. TASK SPONSOR OCAEWC SPO (DMO)	11. NO. OF PAGES 26		12. NO. OF REFERENCES 3
13. URL on the World Wide Web http://www.dsto.defence.gov.au/corporate/reports/DSTO-RR-0295.pdf				14. RELEASE AUTHORITY Chief, Electronic Warfare and Radar Division	
15. SECONDARY RELEASE STATEMENT OF THIS DOCUMENT <i>Approved for public release</i>					
OVERSEAS ENQUIRIES OUTSIDE STATED LIMITATIONS SHOULD BE REFERRED THROUGH DOCUMENT EXCHANGE, PO BOX 1500, EDINBURGH, SA 5111					
16. DELIBERATE ANNOUNCEMENT No Limitations					
17. CITATION IN OTHER DOCUMENTS Yes					
18. DEFTTEST DESCRIPTORS Space-time adaptive processing Airborne radar Target acquisition Covariance					
19. ABSTRACT Pre-built space-time non-adaptive processing (PSTAP) has been proposed in a previous DSTO report. This report further examines the performance of PSTAP using simulated airborne radar data generated by the Rome Laboratory Space-Time Adaptive Processing (RLSTAP) software. Results from the conventional STAP diagonally loaded sample matrix inversion (DL-SMI) method are used as benchmarks to evaluate results of PSTAP. It is found that PSTAP performs the same as STAP. Most importantly, PSTAP does not need computing computationally intensive optimum weights in real-time.					